JOURNAL OF APPLIED ELECTROCHEMISTRY 20 (1990) 916–924

Electrochemistry of anodic fluorine gas evolution at carbon electrodes: Part II Studies on the 'CF' film by the current-interruption, AC impedance, ESCA and Auger Techniques

L. BAI, B. E. CONWAY

Chemistry Department, University of Ottawa, Ottawa, KIN 6N5, Canada

Received 21 January 1990

The 'CF' films that are formed on the surface of carbon anodes used for the fluorine evolution reaction (FER) in KF · 2HF melts at 358 K have been studied by both *in situ* electrochemical current-interruption and a.c. impedance methods, and by *ex situ* surface spectroscopy [ESCA (XPS) and Auger] techniques. The surface analysis measurements indicate that a thin 'CF' (CF_2) film, ~ 1.7 nm in thickness is formed on the carbon anode surface. Results from depth profiling analyses of the film indicate that it is not uniform, higher levels of CF and F components being found towards the carbon anode surface. The *in situ* electrochemical measurements demonstrate that an abnormally small interfacial capacitance, $\sim (1.6 - 2.7) \times 10^{-7}$ F cm^{-2}, arises in the course of the FER at carbon anodes; this was attributed to the presence of a passive dielectric 'CF' film on the carbon electrodes. The determined interfacial capacitance does not change significantly with potential in the potential range studied, which implies that the thickness of the 'CF' film on the fluorine-evolving carbon anodes may be independent of potential.

1. Introduction

The unusually high polarization observed in anodic fluorine evolution at carbon anodes is a problem of considerable commercial significance in fluorine production cell operation and has been quantitatively and reproducibly characterized in our previous publication, Part I of this series [1]. In that paper [1], the origin of the unusually high Tafel slopes and the so-called anode effect was examined and it was suggested that two inter-dependent effects arise: barrier-layer 'CF' film formation; and resulting large fluorine bubble/KF · 2HF melt/carbon anode contact angles leading to an unusual type of gas evolution through a gas film involving adherent lenticular bubbles, well known both in studies and the art of fluorine evolution at carbon anodes.

In the present work, the properties of 'CF' films on carbon anodes have been further examined by both *in situ* electrochemical current-interruption, a.c. impedance methods and their compositions by *ex situ* surface analysis [ESCA (XPS) and Auger] techniques.

The existence of a '$(CF)_x$' film on graphite and carbon anodes was demonstrated by Rüdorf and co-workers already in 1948, using X-ray analysis [2]. Much later, in 1975, Watanabe *et al.* [3] reported that the ESCA spectra of carbon and graphite electrodes, used as anodes for fluorine production from KF · 2HF melts, indicated that a '$(CF)_n$' film was formed on the surface of the electrode. Recently, further studies on the 'CF' films on carbon anodes were carried out by Chemla *et al.* [4, 5] using cyclic-voltammetry and a.c. impedance methods, and by Brown *et al.* [6] using ESCA and SIMS techniques. Other relevant literature was reviewed in Part I.

It has been found by the cyclic-voltammetry method [4–6] that 'CF' films are already almost completely formed (a kind of UPD of fluorine at carbon) even before steady currents for the fluorine evolution reaction (FER) arise. During the FER, behaviour of the 'CF' film was studied by the a.c. impedance method [4, 5]. The 'CF' film, which is a poor conductor, contributes an abnormally small dielectric capacitance (~ 0.2–$0.5\,\mu$F cm^{-2}) which dominates the interfacial capacitance behaviour of melt/carbon interfaces (see below) because it is in series with the higher double-layer capacitance.

However, at high potentials (> 4 V with respect to Cu/CuF_2), the abnormally small capacitance, coupled with an also small Faradaic resistance (which decreases exponentially as potential increases) gives rise to a very small *RC* time constant for the interfacial impedance. Therefore, under these conditions, the true interfacial capacitance cannot be reliably determined, because the high frequency limits of most a.c. impedance equipment are too low to detect, and determine reliably, the abnormally small interfacial capacitance at high anodic potentials (see below).

Brown *et al.* [6] avoided this problem by carrying out all a.c. impedance measurements at a potential

0021-891X/90 $03.00 + .12

(+0.7 V with respect to PdH in KF · 2HF) where no fluorine could occur in their experiments at vitreous carbon electrodes which were pre-polarized anodically at high potentials. However, this method is not exactly a direct '*in situ*' technique.

The current-interruption method is another procedure that has been used to determine interfacial capacitance [7–9]. However, Watanabe *et al.* [7, 8] and Arvia *et al.* [9], using the current-interruption method, found the interfacial capacitance for the FER at carbon electrodes in an anhydrous KF · 2HF melt to be 10^2 times larger than the values reported by Chemla *et al.* [4] using the a.c. impedance method under otherwise comparable conditions.

Therefore, the conditions required for reliable capacitance measurement by the current-interruption method have been examined in the present work. A numerical procedure for data analysis was developed and applied to carbon electrodes evolving fluorine.

Auger surface spectroscopy also was applied, as a supplementary method, in the present work in order to examine the chemical state of the carbon anode surfaces.

2. Experimental details

Most of the experimental details, including the use of carbon rotating cone electrodes (RCE), have been described on the Part I [1]. A Cu/CuF_2 reference and mild steel counter electrodes were employed. Anhydrous KF · 2HF melts (supplied from Eldorado's Laboratory) were used. The cylindrical plexiglass cell (volume 500 cm^3) was mounted in an air-heated oven, operating as a thermostat (±0.5 K) controlled at 358 K. The instrumental arrangement for the current-interruption [10, 11] and a.c. impedance [12] measurements were also as described elsewhere [10–12].

The carbon anode material used in this work was the same as that employed previously, as reported in Part I [1]. This material is porous carbon, supplied by Sers Savoie Carbone, France, as used in plant operation in commercial fluorine production in Eldorado's (Port Hope, Ont.) cells. The electrochemical work described in this paper was carried out on cone electrodes (for rotation, as described in Part I) cut from pieces of the above type of non-graphitic carbon.

The ESCA spectra were obtained on a VG ESCA-III spectrometer using Al Kα and Mg Kα excitation sources. The base vacuum of the spectrometer was 5×10^{-10} Torr. Ion etching was carried out with argon ions (33.5 kV).

The Auger spectra were obtained on a Perkin-Elmer Phi 600 SAM. The electron beam energy used was 3 kV. The analyzer resolution was set at 0.6%. The base vacuum was 1×10^{-9} Torr.

The carbon anode samples for the ESCA and Auger analyses were prepared as follows: a polished [1] carbon electrode was polarized anodically at 0.1 A cm^{-2} (+5.5 V with respect to Cu/CuF_2 in KF · 2HF) for 48 h in the KF · 2HF melt at 358 K. The dimensions of the samples were ~5 mm × 7 mm × 2 mm. The procedure for cleaning the samples was as follows: first the carbon were cleaned ultrasonically in absolute methanol for 5 min. and then sealed in a small glass bottle. Secondly, immediately prior to the ESCA and Auger analyses, the samples were cleaned ultrasonically in distilled water and methanol for 5 min., respectively, and then dried at 393 K for 30 min. The same cleaning procedure was applied to all samples. It was found that control of the cleaning procedure was critical for obtaining reproducible measurements.

3. Results and discussion

3.1. *Current-interruption method*

The current interruption method is used to provide potential-relaxation transients from which the interfacial capacitance is evaluated and compared with data on the same system determined by a.c. impedance spectroscopy.

The theory of the open-circuit potential relaxation or current-interruption method was first treated by Butler and Armstrong [13], based on assumed constancy of the double-layer capacity, C_{dl}, for an ion-discharge process, depolarizing the charged double-layer capacitance. Further developments were made by various authors [14–18], particularly enabling the adsorption behaviour of intermediates in Faradaic reactions to be evaluated through derivation of the electrochemical, potential-dependent, adsorption pseudo-capacitance, C_ϕ [11, 19]. In the present paper, we discuss mainly the *initial* potential-time relaxation behaviour immediately following interruption of the steady-state polarization current. This gives C_{dl}.

3.1.1 Equations and numerical procedure. In order to provide the background for the subsequent discussion of the problem addressed in this paper and analysis of some results, it will be necessary to review, formally, the conventional treatment of open-circuit potential relaxation, following interruption of current.

For an electrode process, the current density, $i(\eta)$, as a function of overpotential, η, is represented by

$$i(\eta) = i_0 \exp(\alpha\eta F/RT) \quad (1)$$

which is the Tafel equation in exponential form and where i_0 is the exchange current density and α the transfer coefficient.

The potential-decay behaviour, after interruption of the polarization current, $i(t = 0)$, is determined by the potential-decay relation [13, 14]:

$$-C\left(\frac{d\eta}{dt}\right) = i(\eta) \quad (2a)$$

$$= i_0 \exp(\alpha\eta F/RT) \quad (2b)$$

where C is the interfacial capacitance ($C = C_{dl}$, if C_ϕ and other incidental capacitances are negligible).

Rearranging Equation 2b gives

$$\eta = \frac{2.3RT}{\alpha F}\log(i_0/C) + \frac{2.3RT}{\alpha F}\log(-d\eta/dt) \quad (3)$$

Integration of Equation 2b (assuming $C \neq f(\eta)$*) gives [7, 8]:

$$\eta(t) = a - b\log(t + \tau) \quad (4)$$

where

$$a = -b\log(2.3i_0/bc) \quad (5)$$

$$b = 2.3\,RT/\alpha F \quad \text{(Tafel slope)} \quad (6)$$

and

$$\tau = bC/2.3i(t = 0) \quad (7)$$

where τ is the integration constant of Equation 2b (*cf.* [14, 18]).

Therefore, both $\log(t + \tau)$ (Equation 4) and $\log(-d\eta/dt)$ (Equation 3) should be linear functions of η (or voltage, V), as is found experimentally [10, 11], and the values of the slopes are numerically the same as the Tafel slope, b, when the condition $C \neq f(\eta)$ is maintained, i.e. mainly when $C_\phi \ll C_{dl}$ although it is well known that C_{dl} may also vary significantly with potential especially around the potential of zero charge in dilute solutions (inapplicable here).

Since $d\eta/dt$ and $i(\eta)$ are experimentally measurable quantities the electrode interface capacitance as a function of η [11, 19] can be obtained directly by means of Equations 2a and 2b:

$$C(\eta) = i(\eta)/(-d\eta/dt) \quad (8a)$$

$$= i_0 \exp(\alpha\eta F/RT)/(-d\eta/dt) \quad (8b)$$

Alternatively,

$$C = i(t = 0)/(-d\eta/dt)_{t=0} \quad (9)$$

is a useful relation, since $i(t = 0)$ can be easily determined experimentally, and C corresponds to the capacitance at the iR–corrected potential at which the initial current is passing. The problem with using Equation 9 is to determine accurately the initial potential–decay slope, $(d\eta/dt)_{t=0}$.

Differentiation of Equation 4 with respect to time, t, gives

$$d\eta/dt = -\frac{b}{2.3(t + \tau)} \quad (10)$$

and

$$(d\eta/dt)_{t=0} = -\frac{b}{2.3\tau}\left(\equiv -\frac{i_{(t=0)}}{C}\right) \quad (11)$$

that is, the initial potential–decay slope, $(d\eta/dt)_{t=0}$ is dependent on the Tafel slope, b, and the integration time-constant, τ.

Since, for an electrochemical activation-controlled process, with $C_\phi \approx 0$, the potential-decay behaviour after interruption of the polarization current must be described by Equation 4, a set of E against t data* can be fitted to Equation 4 by means of the non-linear least squares fitting method which gives the best values for the fitted constants a, b and τ for each set of data. In the present paper, the ASYSTANT software package was used for the non-linear least squares fitting. When the constants b and τ are obtained by the numerical procedures, the initial potential-decay slope can be calculated accurately by means of Equation 11 and then the interfacial capacitance can be derived by using Equation 9.

3.1.2. Testing the method. The numerical procedure described above was applied at first to systems for which the interface capacitances are known. Gold electrodes exhibit no detectable underpotential deposited hydrogen, e.g. as indicated by cyclic-voltammetry measurements [20] nor also any detectable overpotential-deposited hydrogen, as indicated by a.c. impedance [21] and potential-decay measurements [22]. Nickel electrodes, for overpotentials $|\eta| > 0.3$ V for hydrogen gas evolution, also exhibit a constant C_{dl} as indicated by our recent investigations [11]. Thus, the conditions obtaining in the h.e.r. for the above two systems are satisfactory for application of Equation 4 ($C \neq f(\eta)$) and suitable for testing the method described above.

The interfacial capacitance values obtained for each of the above two systems, by applying the described numerical procedure at various $i_{t=0}$ values, are almost constant, $\sim(40\text{–}50) \times 10^{-6}$ F cm^{-2}, a value which can be assigned reasonably to the double-layer capacitance. These results are in good agreement with those obtained in previous studies [11, 22] by applying other techniques.

Specifically, nickel electrodes in the overpotential range $|\eta| > 0.3$ for hydrogen gas evolution exhibit a constant C_{dl} and a potential-dependent pseudo-capacitance in the potential range $0 < |\eta| < 0.3$ V [11]. Therefore, this is a good example which illustrates the case where C measurements for the electrochemical system contain a significant (H) pseudo-capacitance contribution over a certain range of potentials near the hydrogen reversible potential.

3.1.3. Results and discussion for the FER at carbon anodes. Figure 1 shows that the experimentally measured E against $\log t$ plots for relaxation of polarization in the FER at a carbon RCE (rotated at 2500 r.p.m. to facilitate bubble removal [1]) for five initial current-densities (see Table 1). The five lines in Fig. 1 fall on a single line with two negative slopes, $b = -0.80$ and -0.42 V for high η and low η ranges, respectively, when η is plotted against $\log(t + \tau)$ (see eqn. (4)). The slope values (multiplied by -1) are similar to the values of the slopes of the Tafel plots

* In the case of $C = f(\eta)$, e.g. $f(\eta)$ is an exponential function, Equation 4 is formally the same, but with the decay slope $-d\eta(t)/d\log t$ not equal to the Tafel slope (*cf.* [16]).

* From Equation 4: because $\eta = E - E_r = a - b\log(t + \tau)$. Therefore $E = a' - b\log(t + \tau)$, where E_r is the equilibrium potential and $a' = a + E_r$. Since only b and τ are needed for the determination of C [see Equations (9–11)], we can obviously use potential instead of overpotential for the fitting procedure.

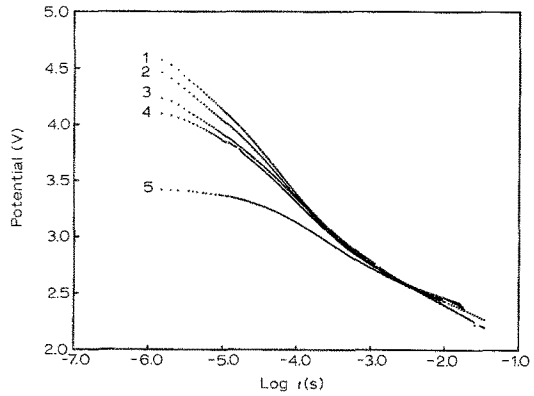

Fig. 1. Experimental potential decay E against log t plots, for the FER at a carbon RCE rotated at 2500 r.p.m. in the KF · 2HF melt at 358 K for five $i(t = 0)$ values: (1) 32; (2) 25; (3) 15; (4) 8.8 and (5) 1.02 mA cm^{-2}.

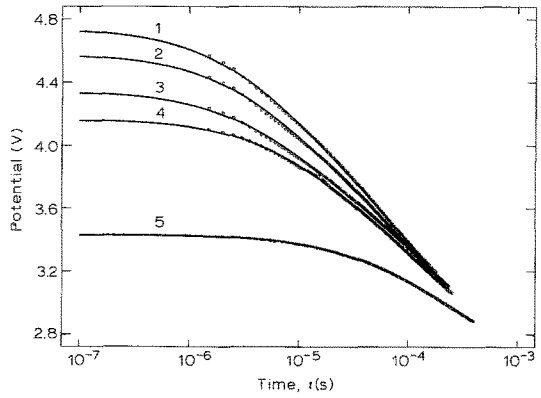

Fig. 2. The experimental initial potential decay plots (points) that are the initial regions of corresponding curves in Fig. 1, and their best fitted curves (solid lines), based on Equation 4. (The resulting best fit parameters of a, b and τ are listed in Table 1).

reported previously [1]. The similar numerical values of the slopes of the Tafel and potential-decay plots imply [13–16] that an effectively constant interfacial capacitance is involved over most of the potential range in the potential relaxation transient.

The initial regions of the potential-decay curves were fitted by the non-linear least squares method using Equation 4. The best fit values of a, b and τ with the resulting interfacial capacitance, C, are listed in Table 1. The experimental data (circle points) with corresponding fitted curves (solid line) are shown in Fig. 2. It is noticed that in Fig. 2 only the data for the initial regions of the decay curves for each experimental potential-decay curve in Fig. 1 were taken for the numerical fitting procedure. This is because Equation 4 is for an electrochemical process exhibiting a single Tafel slope, b, and $i(t = 0)$ and $(-\mathrm{d}\eta/\mathrm{d}t)_{t=0}$, of course, correspond to the initial potential decay behaviour.

The values of $E_{t=0}$ and C in Table 1 are calculated from the a, b and τ parameters for best fit by using Equations 4, 9, 10 and 11, respectively. The remarkable characteristic of the data recorded in Table 1 is the abnormally and consistently low values, (1.6–2.0) × 10^{-7} F cm^{-2}, of capacitances for the melt/carbon interface, which are *two orders of magnitude* lower than for a normal aqueous solution/metal electrode interface (see 3.1.2) and for the C results of Watanabe [7, 8] and Arvia [9].

These abnormally low C values are believed [4, 6] to arise because of the formation of a passivating layer of 'CF' species having poor conductivity which introduces an additional low dielectric capacitance *in series* with the larger double-layer capacitance, so that it is the low dielectric capacitance which determines the overall measured C. Also, it is the effect of this film, behaving non-ohmically (*cf.* [20] and [23]), that gives rise to abnormally high Tafel slopes for the FER at carbon electrodes [1] through the well known activated charge-transport mechanism [23].

However, the values of interfacial capacitance reported for carbon electrodes at which the FER is proceeding in KF · 2HF melts are about 5.0 × 10^{-5} F cm^{-2} as determined by the current-interruption method in two previously published works [7, 9]. Thus, abnormally small C values for carbon electrodes under FER conditions were not detected, although a method similar, in principle, to that used here had been employed.

Therefore, the conditions required for reliable C measurement by the current-interruption method have to be examined carefully. The main question is how $(\mathrm{d}\eta/\mathrm{d}t)_{t=0}$ can be accurately measured at $t = 0$, when using Equations (9–11). This problem can be illustrated as in Fig. 3.

Figure 3 shows calculated η against log $(-\mathrm{d}\eta/\mathrm{d}t)$ and log t plots, using Equations 3 and 4, taking i_0 =

Table 1. Experimental values of i(t = 0), *and the best fit values of* a, b, τ *with* E(t=0) *and* C *for the data shown in Fig.* 2

	$i_{t=0}$ (mA cm^{-2})	$E_{t=0}$ (V)	a (V)	b (V)	τ (s)	C(F cm^{-2})
1	32	4.74	0.152	0.810	2.20 × 10^{-6}	2.0 × 10^{-7}
2	25	4.58	0.346	0.755	2.51 × 10^{-6}	1.9 × 10^{-7}
3	15	4.34	0.774	0.645	2.93 × 10^{-6}	1.6 × 10^{-7}
4	8.8	4.16	0.642	0.672	5.74 × 10^{-6}	1.7 × 10^{-7}
5	1.02	3.43	1.268	0.479	33.9 × 10^{-6}	1.6 × 10^{-7}

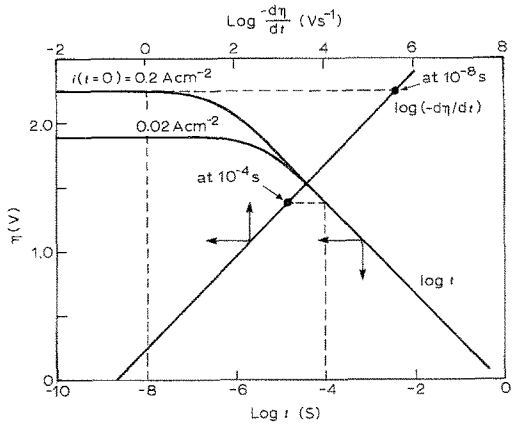

Fig. 3. Calculated overpotential η against log $(-\mathrm{d}\eta/\mathrm{d}t)$ and η against log t plots, using Equations 3 and 4, taking C = 0.5 × 10^{-6} F cm^{-2}, α = 0.2, T = 358 and i_0 = 1 × 10^{-7} A cm^{-2} for two $i(t = 0)$ values of 0.2 and 0.02 A cm^{-2}. The points and dashed lines on the log $(-\mathrm{d}\eta/\mathrm{d}t)$ plot indicate the values of log $(-\mathrm{d}\eta/\mathrm{d}t)$ at potential decay times 10^{-4} and 10^{-8} s, respectively, for the potential-decay curve for $i(t = 0)$ = 0.2 A cm^{-2}.

1×10^{-7} A cm^{-2}, $C = 0.5 \times 10^{-6}$ F cm^{-2}, $\alpha = 0.2$ and $T = 360$ K, for $i(t = 0) = 0.2$ and 0.02 A cm^{-2}, a condition close that arising with the FER at carbon electrodes. This figure shows that from the time range 10^{-10}–10^{-7} s, ($t \leqslant 10^{-7}$ s), corresponding to the initial flat region of the potential relaxation transient (i.e. when $t \ll \tau$ in Equation 4), both η and $(-d\eta/dt)$ do not change significantly with time. After 10^{-6} s, however, η and log $(-d\eta/dt)$ change linearly with log t. Hence, to determine C by using Equations 9–11, $(d\eta/dt)_{t=0}$ must be taken at least within 10^{-7} s of interruption of current for $i(t = 0) > 0.02$ A cm^{-2}. Thus, it can be understood how Watanabe *et al.* [7] and Arvia and Cusminsky [9], measuring C by using Equation 9 and recording potential decay transients by means of an analogue oscilloscope screen taking 10^{-4} s as their practical limit for $t \longrightarrow 0$, found a value of C about 10^2 times larger than it should have been (since, $-d\eta/dt$ at 10^{-4} s is $\sim 10^2$ times smaller than it should have been; see Fig. 3).

In this case, it is evident that the correct value of $(d\eta/dt)$ for $t \longrightarrow 0$ must be obtained by a numerical procedure of extrapolation, e.g. as described above. Therefore, the previously reported [7, 9] interfacial capacitance values must be regarded as doubtful results, even with respect to magnitude.

3.2. *Results from a.c. impedance measurements*

Figure 4 shows the a.c. impedance data, plotted in the complex-plane for the FER at the carbon RCE, rotated at 2000 r.p.m., for the following anode potentials: (1) 3.90, (2) 3.80, (3) 3.72 V with respect to Cu/CuF_2 in the melt.

The impedance spectra in Fig. 4 have the standard form of single semi-circles with some part of the sector in the high frequency range missing. This is because, of a very small interfacial capacitance (as in Table 1) and also a relatively small Faradaic resistance, R_f, the 10 kHz high-frequency limit of the Solartron 1170 instrument is then too low for the full semi-circle to be traced to the high-frequency intercept of the curve. For higher potentials, R_f becomes exponentially smaller (according to a Tafel-type relation) so that complete semi-circles will not be able to be followed.

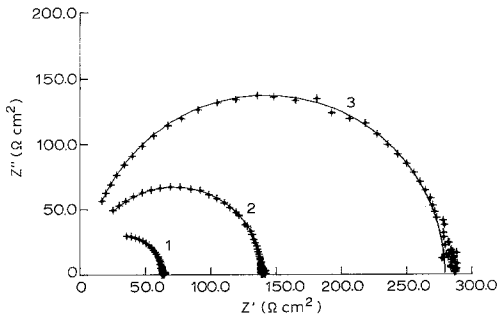

Fig. 4. The a.c. impedance data (+ points), plotted in the complex plane for the FER at the carbon RCE (rotated at 2500 r.p.m.) at anodic potentials (1) 3.90; (2) 3.80 and (3) 2.72 V with respect to Cu/CuF_2. The solid lines are the corresponding simulated curves using Equation 12 and the values of R_f and C in Table 2.

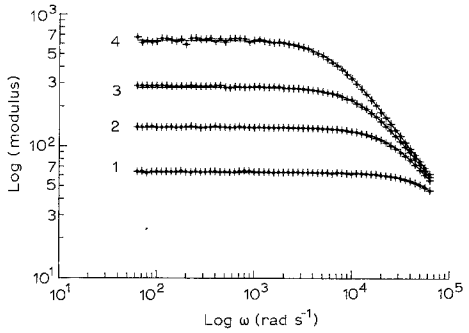

Fig. 5. Experimental (× points) and simulated (solid lines) Bode plots, log $|Z|$ against log ω, for the FER at carbon RCE (rotated at 2500 r.p.m.). Curves 1, 2 and 3 represent the same data as those of Fig. 4; curve 4 is for and anodic potential of 3.63 V with respect to Cu/CuF_2. The values of R_f and C for the simulation curves are as listed in Table 2.

For example, on curve 1 for 3.9 V, only half of the semi-circle can be seen with a high-frequency limit of 10 kHz. At higher potentials, $E \geqslant 4.0$ V, no significant impedance spectra can be gathered since only a very small part of the semi-circles can be observed with the Solatron 1170 instrument used.

The frequency dispersion of the data in Fig. 4 are shown as Bode plots in Fig. 5. Curves 1, 2 and 3 in Fig. 5 represent the same data as shown correspondingly in Fig. 4. Curve 4 in Fig. 5 is for the impedance data at an anodic potential of 3.63 V, with respect to Cu/CuF_2.

The standard semi-circles in the complex-plane plots (Fig. 4) and a slope of -1 in the high-frequency range with a slope of 0 in the low-frequency range of the Bode plots (Fig. 5) indicates that the equivalent circuit for the present situation at carbon is an interfacial capacitance*, C, in parallel with a Faradaic resistance R_f. The impedance of the circuit as a function of frequency is then given by:

$$Z = Z' - jZ'' \tag{12}$$

where

$$Z' = R_f/(1 + \omega^2 C^2 R_f^2) + R_s$$

$$Z'' = \omega C R_f^2/(1 + \omega^2 C^2 R_f^2)$$

and where R_s = ohmic solution resistance between the reference and working electrodes.

With progression of the frequency scan, it is to be noted that no second semi-circle arises. This indicates, except under some special conditions, absence of a significant pseudo-capacitance for electroactive chemisorbed F species at appreciable coverage. (The F in the 'CF' film is thus to be regarded as irreversibly deposited, thus constituting a non-electroactive species in this sense, so that the 'CF' film acts simply as an extra dielectric electrostatic capacitance. This is consistent with the known chemical inactivity of C–F bonds.)

* Since the much smaller dielectric capacitance due to the 'CF' film is in *series* with the double-layer capacitance, the total interfacial capacitance should be approximately equal to the much smaller dielectric 'CF' film capacitance, as noted earlier.

Table 2. Values of the R_f and C parameters for simulation of the experimental a.c. impedance behaviour of Figs. 4 and 5, using Equation 12 ($R_s = 4.5\,\Omega cm^2$).

	Potential (*V*)	R_f (Ωcm^2)	*C* ($F cm^{-2}$)
1	3.90	59	2.5×10^{-7}
2	3.80	135	2.7×10^{-7}
3	3.72	275	2.7×10^{-7}
4	3.63	632	2.6×10^{-7}

The R_f and C parameters required for simulation of the experimental data in Fig. 5, using Equation 12, are listed in Table 2. The solid lines in Figs. 4 and 5 are the corresponding curves for simulation of the experimental results using the values of R_f and C in Table 2.

Again, an abnormally small interfacial capacitance, $\sim(2.5\text{–}2.7) \times 10^{-7}\,F\,cm^{-2}$, is determined for the FER at carbon anodes by the a.c. impedance method (see Table 2). These values are only slightly different from those obtained by the current-interruption method (see Table 1). Therefore, these results should be considered as reliable since they were determined by two completely independent methods.

The significant conclusions that can be drawn from the interfacial capacitance measurements made by means of the current-interruption and a.c. impedance methods are that the apparent interfacial capacitance for carbon electrodes at which anodic fluorine evolution is proceeding in anhydrous KF · 2HF at 358 K is abnormally small, $\sim(1.6 - 2.7) \times 10^{-7}\,F\,cm^{-2}$ over the potential range studied; this is attributed to the presence of a passive dielectric 'CF' film on the carbon electrodes, which introduces a low capacitance in series with the normal double-layer capacitance of the carbon/melt interface. The values of the interfacial capacitance do not change significantly with potential (see Tables 1 and 2); in other words, the thickness of the 'CF' film is more or less independent of potential. This is in agreement with the conclusion drawn from the kinetic experiments that the constancy of Tafel slopes observed [1] over an appreciable logarithmic range of i implies a constant width of the 'CF' film barrier for the electron charge-transfer process of discharge of F from HF or F^-. It is significant that the 'CF' film does not seem to thicken with increasing positive potential like oxide films do on metals. We suggest that this difference arises because the F is *covalently* bound to the carbon surface so cannot undergo the process of 'place-exchange' thickening or cation injection into the growing film that characterizes the mechanism and kinetics of oxide-film growth on metals.

3.3. *ESCA Results*

Figure 6 shows the wide survey scan ESCA spectrum of a carbon anode surface that had been previously used for fluorine evolution. The main components of the spectrum are peaks corresponding to transitions at carbon and fluorine atoms, with an oxygen peak due

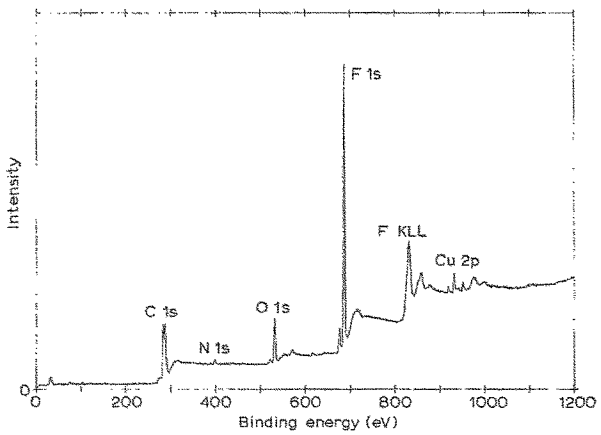

Fig. 6. Wide survey scan ESCA spectrum of the surface of a carbon anode used for fluorine gas evolution in the KF · 2HF melt.

to the presence of residual H_2O, MeOH or CO on the surface. The formation of the CF film on carbon anodes is indicated by the presence of a strong F 1*s* peak and, especially, the splitting of the C 1*s* peaks shown in Fig. 6. A detailed spectral scan of the C 1*s* region is shown in Fig. 7 from which it is seen that the experimental C 1*s* peaks (+points) are actually resolvable into four components which correspond to 'CC', 'CO', 'CF' and 'CF_2' states of C at binding energies of 284.0, 285.5, 288.2 and 291.0 eV, respectively [24]. The area under each peak represents the relative contribution of each component. The broad 'CF_2' peak in Fig. 7 may be compounded from 'CF_2', 'CF_3', etc., components on the oxidized carbon surface.

The assignment of the CF and CF_2 peaks in Fig. 7 was made according to the principles discussed by Thomas *et al.* [24], who determined that the surface groups CF, CF_2 and CF_3 exhibited chemical shifts from the main graphite C 1*s* peak of 4.7, 6.7 and 9.0 eV, respectively. Therefore, the chemical state of the fluorocarbon species in Fig. 7 should be mainly CF with some 'methylenic' type CF_2.

It is to be noted that the strong C 1*s* peak at 284.0 eV, seen in Fig. 7, does not necessarily mean that 'free carbon' exists in a great proportion of the top layer of a used carbon anode surface. Because the electron escape depth from carbon is about 2 ~ 4 nm

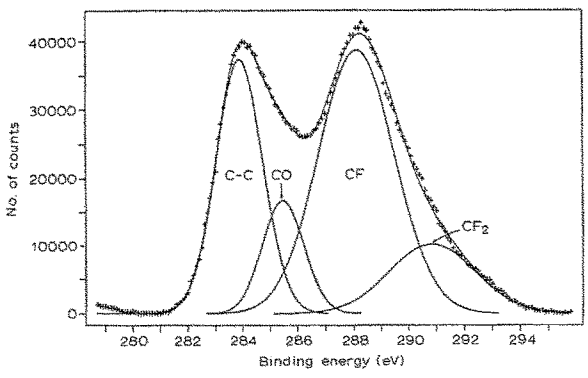

Fig. 7. Experimental (× points) and computer fitted and deconvoluted curves (solid lines) for detailed ESCA scan of C 1*s* peaks for a carbon anode used for anodic fluorine gas evolution in the KF · 2HF melt.

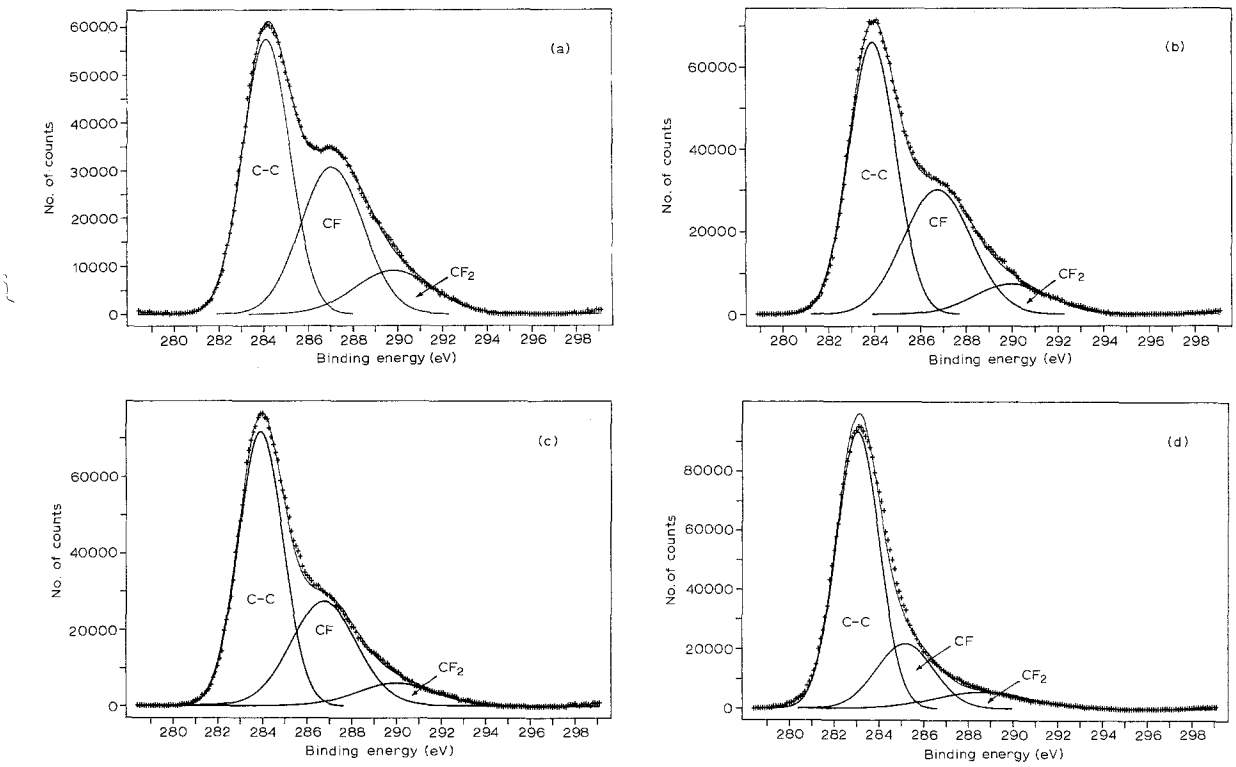

Fig. 8. Experimental (× points) and computer fitted and deconvoluted curves (solid lines) of ESCA C 1*s* peaks for a carbon anode used for anodic fluorine gas evolution after sputtering for (a) 5; (b) 10; (c) 20 and (d) 600 s, respectively.

for Mg Kα X-rays [25] and the thickness of the 'CF' film determined by the ion etching technique in the present work (see below) and that of others [6] is about 1.0 ~ 2.0 nm, the strong C 1*s* peak at 284.0 eV most probably contains a contribution from bulk carbon beneath the thin 'CF' film. Also, the Auger results (see below) indicate that the F content is uniform on areas all over the flat anode surfaces.

3.3.1. Ion sputtering. Depth profiling of carbon anodes surfaces can be accomplished by controlled erosion of the surface by ion sputtering. The detailed C 1*s* region profiles for a used carbon anode surface after ion sputtering for, typically (a) 5, (b) 10, (c) 20, (d) 600 s, respectively, are shown in Fig. 8 where the cross points represent the experimental data and solid lines are the computer-fitted and deconvoluted curves. It was found that no 'CO' component was detectable in the C 1*s* profile after the samples had been ion sputtered (see Fig. 8).

From the ion sputtering data, the thickness of the 'CF' film on the carbon anodes can be calculated, based on a thin-film model [26]. The inelastic mean free path for a C 1*s* photoelectron was taken as 2.7 nm as usually assumed. The depth profiling for the surface atom fractions of C–C, CF (CF_2), F and O can also be calculated from their ESCA 1*s* peaks in the ion sputtering data, taking the relative sensitivity factor [27] S = 1.0, 0.205 and 0.63 for F, C and O, respectively. The surface atom fractions of CC, CF, F and O and the CF film thickness are then determined as listed in Table 3.

It is noticed that appreciable 'F' and 'CF' contents still apparently exist on the carbon sample surface even after 600 s sputtering. A blank carbon sample was therefore tested, which was cut from inside the bulk of a used carbon anode and had never been in contact directly with the KF · 2HF melt. It was found that a similar amount of 'CF' and 'F' was detected on this blank carbon sample as in Fig. 8d. These results suggest that some fluorine gas may pass through the pores inside the bulk carbon anodes during anodic

Table 3. The atom fractions and 'CF' film thickness of species generated at a used carbon anode surface from ESCA ion sputtering measurements

Surface atom fraction (%)	*Sputtering time(s)*							
	0	5	10	15	20	40	120	600
C–C	27	47	56	58	60	65	73	84
$CF(CF_2)$	32	20	18	17.8	17	15	12	8.9
F	33	26	21	19	18	16	12	5.6
O	8.6	6.1	5.1	4.8	4.5	4.2	3.4	1.9
Film thickness (nm)	1.77	0.87	0.54	0.51	0.42	0.33	0.25	~0

fluorine evolution as was demonstrated previously [28]. Therefore, for the calculation of the 'CF' film thickness, the intensity of the C 1*s* (284.0 eV) signal after 600 s sputtering time was taken as the 'bulk' carbon value.

From the ion sputtering results listed in Table 3, it can be concluded that a very thin 'CF' ('CF_2') film, ~ 1.7 nm in thickness can be detected on the carbon anode surface that had been used for fluorine gas evolution. The depth profiling of the film is not, however, uniform, higher 'CF' and 'F' contents being found towards the carbon anode surface.

3.4. *Auger surface analyses*

The main purpose of applying Auger analysis was to examine the compositional uniformity of the surfaces of the carbon anodes. Owing to the nature of the ESCA method, ESCA results represent the average values over the total surface (5 mm × 7 mm) of the sample. The advantage of the Auger method is that a very small area, e.g. a spot 1 μm in diameter, can be examined.

However, a substantial problem was met in applying Auger analysis to examine quantitatively the 'CF' film on the carbon anodes: the electron beam seriously interfered with the fluorine signal due to damage to the fluorinated surface. Even though the beam current was reduced to minimum values of 1–0.5 nA and data acquisition was performed while rastering the electron beam at 3000–10000 × magnification to average the signal from a small area, in all cases, some visible beam damage had occurred during data acquisition, as was confirmed by the series of multiplex spectra. However, it was still possible to check the surface uniformity and semi-quantitatively the surface content of fluorine on various carbon anode samples.

A typical Auger survey spectrum of a used carbon anode sample taken on a smooth element of area was shown in Fig. 9 where only two peaks are, as expected, recognizable; these are for carbon and fluorine, respectively. The existence of the 'CF' film on the carbon anodes is thus beyond any doubt.

The percentage values of the elements carbon and fluorine in the surface film, determined by the Auger analyses, are listed in Table 4.

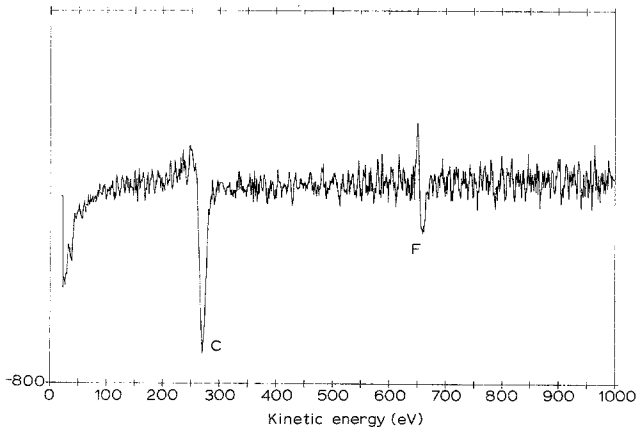

Fig. 9. Auger spectrum for a carbon anode used for anodic fluorine gas in the KF · 2HF melt.

Table 4. Percentage values of C and F on a carbon anode surface

Beam current (nA)	*Raster*	*Location*	*C*	*F*
5	3000 ×	flat area	73.5	26.4
1	3000 ×	flat area	66.8	33.1
0.5	3000 ×	flat area	62.6	37.3
0.5	3000 ×	in a hole	82.9	17.0

Data acquisition for provision of the information in Table 4 was performed on a new area of the sample for each measurement. The apparent F content increases from 26.4 to 37.3% as the beam current decreases from 5 to 0.5 nA. Therefore, the actual F should be somewhat higher than 37.3% for the surface of a carbon anode used for F_2 evolution.

The F content in a hole is less than half that on flat surface regions. This may imply that the local current density in the holes was substantially lower than that in the flat surface regions. Comparatively, it was found that the F content values on different surface regions were very similar, i.e. F content is more or less unifom on the flat areas all over the anode surface.

4. Conclusions

1. Application of two *in situ* electrochemical techniques, current-interruption and a.c. impedance methods, showed that an abnormally small interfacial capacitance, $\sim(1.6\text{–}2.7) \times 10^{-7}$ F cm^{-2}, arises at carbon anodes at which fluorine gas is anodically evolved from KF · 2HF melts. This can be attributed to the presence of a passive dielectric 'CF' film on the carbon electrodes.

2. Two *ex situ* surface spectroscopy techniques, ESCA and Auger, demonstrated that a thin 'CF'('CF_2') film, ~ 1.7 nm in thickness is formed on the carbon anode surface. The results of ESCA depth profiling analyses showed that the film is, however, not uniform, higher 'CF' and F contents being found towards the carbon electrode surface.

Acknowledgements

Grateful acknowledgement is made to the Natural Sciences and Engineering Research Council of Canada for support of this work on a joint project with Eldorado Resources, Ltd. (now Cameco — A Canadian Mining and Energy Corporation, formerly Eldorado Resources Ltd.) Special thanks are due to Dr. T. Zawidzki, formerly of Eldorado, for many stimulating discussions during this research project and for his support during its execution. We also thank Dr. D. Creber of Alcan International, Kingston, for carrying out the ESCA and Auger experiments.

References

[1] L. Bai and B. E. Conway, *J. Applied Electrochem.* **18** (1988) 839.

[2] W. Rüdorff, U. Hofmann, G. Rüdorff, J. Endell and G. Ruess, *Z. Anorg. Allgem. Chem.* **256** (1948) 125.
[3] H. Imoto, T. Nakajima and N. Watanabe, *Bull. Chem. Soc. Japan* **48** (1975) 1633.
[4] M. Chemla, D. Devilliers and F. Lantelme, in Proceedings of the First International Symposium on Molten Salt Chemistry and Technology, Kyoto, Japan, April 1983; see also *Ann. Chim. Fr.* **9** (1984) 633.
[5] D. Devilliers, F. Lantelme and M. Chemla, *Electrochim. Acta* **31** (1968) 1235.
[6] O. R. Brown, B. M. Ikeda and M. J. Wilmott, *ibid.* **32** (1987) 1163.
[7] N. Watanabe, M. Inoue and S. Yoshizawa, *J. Electrochem. Soc. Japan.* **31** (1963) 168.
[8] N. Watanabe, *J. Fluorine Chem.* **22** (1983) 205.
[9] A. J. Arvia and J. B. de Cusminsky, *Trans. Faraday Soc.* **58** (1962) 1019.
[10] B. E. Conway, L. Bai and D. F. Tessier, *J. Electroanal. Chem.* **161** (1984) 39.
[11] B. E. Conway and L. Bai, J. Chem. Soc., *Faraday Trans. I* **81** (1985) 1841.
[12] L. Bai, D. A. Harrington and B. E. Conway, *Electrochim. Acta* **32** (1987) 1713.
[13] J. A. V. Butler and G. Armstrong, *Proc. Roy. Soc., Lond.* **A137** (1932) 604; see also *Trans. Faraday Soc.* **29** (1933) 1261.
[14] H. B. Morley and F. E. W. Wetmore, *Can. J. Chem.* **34** (1956) 359.
[15] V. I. Past and I. Jofa, *Zh. Fiz. Khim.* **33** (1959) 913 and 1230.
[16] B. E. Conway and P. L. Bourgault, *Can. J. Chem.* **27** (1957) 292; see also *Trans. Faraday Soc.* **58** (1962) 593.
[17] T. Anderson and H. Eyring, *J. Phys. Chem.* **67** (1963) 92.
[18] B. V. Tilak and B. E. Conway, *Electrochim. Acta* **21** (1976) 745.
[19] B. E. Conway and L. Bai *J. Electroanal. Chem.* **198** (1986) 149.
[20] B. E. Conway, H. A. Kozlowska, B. Barnett and J. Mozota, *ibid.* **100** (1979) 417.
[21] G. J. Brug, M. Sluyters-Rehbach and J. H. Sluyters, *ibid.* **181** (1984) 245.
[22] B. E. Conway and L. Bai, *Electrochim. Acta* **31** (1986) 1013.
[23] R. E. Mayer, *J. Electrochem. Soc.* **107** (1960) 847.
[24] P. Cadman, J. D. Scott and J. M. Thomas, *Surface Sci.* **15** (1977) 75.
[25] C. J. Powell *ibid.* **44** (1974) 29.
[26] J. S. Hammond and N. Winograd, in 'Comprehensive Treatise of Electrochemistry', vol. 8, (edited by R. E. White, J. O'M. Bockris, B. E. Conway and E. Yeager), Plenum, New York (1984).
[27] J. H. Schofield, *J. Electronic Spectroscopy* **8** (1976) 129.
[28] D. M. Novak and P. T. Hough, Report to Eldorado Resources Ltd., Ottawa, private communication (1984).